# The Effect of Clay Modification on the Mechanical Properties of Poly(methyl methacrylate)/ Organomodified Montmorillonite Nanocomposites Prepared by In Situ Suspension Polymerization

**Xiang Wang, Qiang Su, Jiahui Shan, Junping Zheng**
*Tianjin Key Laboratory of Composite and Functional Materials, School of Materials Science and Engineering, Tianjin University, Tianjin 300072, People's Republic of China*

**Poly(methylmethacrylate) (PMMA)/montmorillonite (MMT) nanocomposites were prepared by in situ suspension polymerization. MMT was previously organically modified by different modification agents [dioctadecyl dimethyl ammonium chloride (DODAC) and methacrylatoethyltrimethyl ammonium chloride (MTC)] and different modification method (cation-exchange reaction and grafting reaction), ultimately giving rise to five kinds of organomodified MMT (OMMT). The structure of the OMMT was studied by Wide angle X-ray diffraction (WAXD) and Fourier transform infrared spectroscopy (FTIR). Meanwhile, the structure of the PMMA/MMT nanocomposites microspheres was also investigated by WAXD. The molecular weight of the polymers extracted from PMMA/MMT nanocomposites was measured by gel permeation chromatograph (GPC). Finally, the mechanical properties of these PMMA/MMT nanocomposites were studied in detail. It was found that large interlayer spacing ($d_{001}$) of OMMT could not entirely ensure an exfoliated structure of resultant PMMA/MMT nanocomposites, while OMMT with relative small $d_{001}$ could still yield exfoliated structure as long as the compatibility between OMMT and polymer matrix was favorable. In addition, the results of mechanical investigation indicated that the compatibility between OMMT and PMMA matrix turned out to be the dominant factor deciding the final mechanical properties of PMMA/MMT nanocomposites. POLYM. COMPOS., 00:000–000, 2014.**


## INTRODUCTION

The development of strategies for the synthesis of polymer/clay nanocomposites is rapidly growing mainly because of enhanced properties emerging from such kind of materials [1–7]. Among the different types of clay, montmorillonite (MMT) is the most used nanofiller because of its natural abundance and high aspect ratio [8]. MMT has excellent capability to exfoliate and disperse within polymer matrices, therefore polymer/MMT nanocomposites have been studied extensively in recent years [9–12].

Among various polymer matrices, poly(methylmethacrylate) (PMMA) is considered to be a good host material for polymer/MMT nanocomposites due to its outstanding dimensional stability, outdoor weather resistance, and good mechanical strength [13–15]. Compared with neat PMMA, the obtained PMMA/MMT nanocomposites exhibited several favorable properties such as enhanced mechanical properties, higher glass transition temperature, better thermal stability and fire retardancy, and improved solvent resistance and anticorrosion ability [16–22]. Such advantages make PMMA/MMT nanocomposites a promising kind of composite materials with potential applications in many fields.

Numerous tactics have been implemented to prepare PMMA/MMT nancomposites, such as in situ polymerization, melt intercalation and solution cast method [23–27]. For in situ polymerization, dispersion of the filler is performed in the monomer or pre-polymer stage before initiating polymerization. Therefore, this method has the advantage of improved dispersion and integration between the phases [28]. In the case of PMMA, in situ polymerization can be accomplished by bulk polymerization, solution polymerization, emulsion polymerization and suspension polymerization [23–25, 29–31]. PMMA prepared by suspension polymerization could be easily processed by injection molding or extrusion molding, which makes possible to produce PMMA products with varied shapes and, therefore, makes suspension polymerization one of the two main methods to produce PMMA largescalely in contemporary chemistry industry. In addition, suspension polymerized PMMA have been extensively applied in biomedicine fields such as dentures [32],

*Correspondence to*: Junping Zheng; e-mail: jpzheng@tju.edu.cn
Contract grant sponsor: National Natural Science Foundation of China; contract grant number: 51473114; contract grant sponsor: Program for New Century Excellent Talents in University, People's Republic of China.
DOI 10.1002/pc.23343
Published online in Wiley Online Library (wileyonlinelibrary.com).

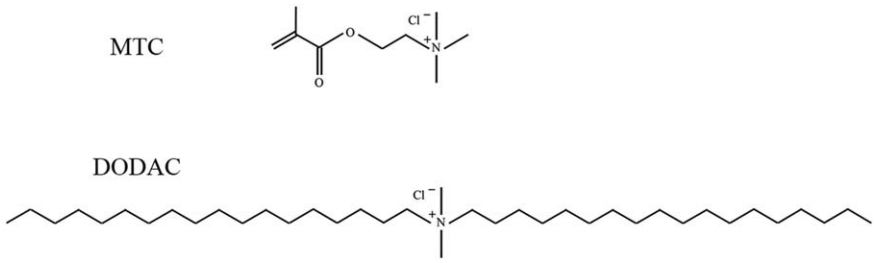


FIG. 1. Chemical structure of organomodifiers.

surgical bone cements [33], drug delivery systems [34] and so on. The incorporation of MMT into suspension polymerized PMMA surely would have some beneficial impact on various properties and give birth to a promising category of novel composite materials.

However, such kind of PMMA/MMT nanocomposites reported in the open literature so far were mainly prepared by simply adding MMT clays into commercially available suspension polymerized PMMA through melt intercalation or during curing process [35–38], yet the studies of PMMA/MMT nanocomposites prepared by in situ suspension polymerization are scarcely reported. In 2001, Huang *et al*. first reported the synthesis of PMMA/MMT nanocomposites by in situ suspension polymerization and an improvement of thermal stability was observed [39]. Clarke and his coworkers also synthesized a series of PMMA/MMT nanocomposites by in situ suspension polymerization. In their work, the effect of the clay on the molecular weight and rheology behavior of the polymer matrix was studied [40]. In our recent work, we also explored the biocompatibility and thermal stability of PMMA/MMT denture base material prepared by in situ suspension polymerization [41, 42]. Unfortunately, to the best of our knowledge, there are no specialized reports on the mechanical properties of PMMA/MMT nanocomposites prepared by in situ suspension polymerization, which may hamper further study and application of these materials since mechanical properties are one of the most important performances for nanocomposites.

Therefore, in this article, we aim to focus on the mechanical properties of PMMA/MMT nanocomposites synthesized by in situ suspension polymerization. Five different kinds of organomodified MMT (OMMT) were prepared by utilizing different modification agents and different modification methods. Wide angle X-ray diffraction (WAXD) and Fourier transform infrared spectroscopy (FTIR) were applied to study the structure of OMMT. Meanwhile, the structure of the PMMA/MMT nanocomposites was also investigated by WAXD. The molecular weight of the polymers extracted from PMMA/MMT nanocomposites was measured by gel permeation chromatograph (GPC). At last, the mechanical properties of resultant PMMA/MMT nanocomposites were evaluated and the effect of clay modification on the mechanical properties of final nanocomposites was discussed.

## EXPERIMENTAL

### *Materials*

Methyl methacrylate (MMA, analytical grade) was purchased from Tianjin Kermel Chemical Reagent Co. (Tianjin,China) and purified by the standard treatment with aqueous 5% NaOH followed by distillation at a normal pressure to remove inhibitor and then stored at low temperature before use. Sodium montmorillonite (Na-MMT, CEC: 90 meq/100 g) was supplied by Huate Chemical Co. (Zhejiang, China). Dioctadecyl dimethyl ammonium chloride (DODAC) was supplied by Xiamen Pioneer Technology Co. (Fujian, China). Methacrylatoethyltrimethyl ammonium chloride (MTC) was supplied by Xinyu Chemical Co. (Zhejiang, China). All other reagents were of analytical grade. Distilled water was used throughout.

### *Preparation of OMMT*

The OMMT was prepared by a cation-exchange reaction between the sodium cations of MMT clay and quaternary alkylammonium cations. MMT aqueous suspension (1 wt%) was ultrasonically dispersed, and then the dispersion was added to a three-neck flask. Three different kinds of aqueous solutions (containing MTC, DODAC, and the mixture of MTC and DODAC (mass ratio = 1:1), respectively), pH of which was adjusted to 3-4 with hydrochloric acid beforehand, were added dropwise under continuous agitation respectively. The mixture was stirred at 80°C for 1 h. The results were filtered, separated and then dried at 60°C to obtain OMMT named as M-MMT, D-MMT and MD-MMT, standing for MMT modified by MTC, DODAC, and the mixture of MTC and DODAC, respectively. The chemical structures of modifiers are illustrated in Fig. 1.

PMMA can be grafted onto modified MMTs for the existence of unreacted double bond of MTC. The grafting process is described below: xylene (150 mL) was mixed with M-MMT (2.5 g) and MD-MMT (2.5 g), respectively, and then the mixture was ultrasonically dispersed. The mixture was placed into four-neck flask equipped with mechanical stirrer under a slow stream of $N_2$ and then heated to 80°C, followed by adding benzoyl peroxide

 DOI 10.1002/pc

(BPO) initiator (0.2 g). The system was maintained for 30 min to obtain a homogeneously dispersed system and then MMA (20 mL) was added dropwise into the mixture system. After the addition was completed, the reaction was performed for 6 h under stirring, and then cooled to room temperature. The results were filtered, separated, washed and then dried at 60°C for 24 h to obtain modified MMT denoted as PgM-MMT and PgMD-MMT, standing for PMMA grafted M-MMT and MD-MMT, respectively.

### *Preparation of PMMA/MMT Nanocomposites Via In Situ Suspension Polymerization*

PMMA/MMT nanocomposites were prepared by in situ suspension polymerization. A typical synthesis process was described as follows: the mixture of OMMT (0.6 g) and MMA monomer (60 mL) was ultrasonically dispersed, then diluted with distilled water (180 mL) containing hydroxylethyl cellulose (HEC, 1.8 g) used as dispersant and sodium dodecyl benzene sulfonate (SDBS, 0.072 g) used as surfactant, stirring until obtaining homogeneous suspension system. The mixture was poured into the suspension polymerization reactor and then heated to 75°C, bubbled with nitrogen for 30 min under agitation. After initiator (BPO, 0.6 g) was employed to the system, the reaction was performed for 12 h under continuous nitrogen flow. The reaction products were repeatedly washed with water, filtered and then dried in a vacuum oven overnight at 60°C to obtain PMMA/M-MMT, PMMA/D-MMT, PMMA/MD-MMT, PMMA/PgM-MMT, and PMMA/PgMD-MMT, standing for nanocomposites with M-MMT, D-MMT, MD-MMT, PgM-MMT, and PgMD-MMT.

### *Preparation of Specimens for Mechanical Tests*

Obtained nanocomposite microspheres were mixed with MMA by the mass ratio of 1:1 and introduced into the resin dough, which then was put into the mold and pressed in a pressing apparatus. The mold was placed in water and maintained at 60°C for 1.5 h, then rapidly heated to 100°C and maintained for another 1 h before being taken out of water. Finally the specimens were removed and polished, which were used for further mechanical tests after cooling to room temperature. The standard of tensile specimens was 50 mm × 7 mm × 2 mm and that of flexural specimens was 64 mm × 10 mm × 3.3 mm.

### *Polymer Extraction*

A reverse of cationic-exchange reaction was employed to separate bound PMMA from the inorganic component in the nanocomposites [16]. The typical extraction procedure is as follows. As-synthesized PMMA/MMT nanocomposites powder of 3 g was treated with soxhlet extraction at 80°C for 48 h. The solvent used was acetone. Then the extraction product was determined by GPC with THF as the eluent.

### *Characterization*

For the confirmation of successful modification of OMMT, The FTIR spectra of the samples were taken with a Nicolet Magna Nicolet-5DX FTIR spectrophotometer with a resolution of 4 $cm^{-1}$ and 32 scans in the range of 4,000–400 $cm^{-1}$ using KBr pellets.

WAXD was used to characterize the OMMT and dispersion of OMMT in the nanocomposites microspheres, which was performed by using Rigaku D/MAX-2500 diffractometer with Cu Kα radiation ($\lambda$ = 0.154 nm) at a generator voltage of 50 kV and a generator current of 180 mA, scanning over the 2θ range from 1° to 30° at a scanning rate of 2°/min.

The molecular weights of PMMA extracted from PMMA/MMT nanocomposites were analyzed by GPC using THF as eluent. The instrument was equipped with a Waters 1515 pump, a Waters 2414 refractive index detector and three Shodex-Gel linear columns. The calibration was based on polystyrene standards with a narrow molecular weight distribution.

The tensile tests of the specimens were carried out at room temperature by using a Testometric Universal Tester M350-20kN at a crosshead speed of 2 mm/min. At least five specimens were tested for each sample and mean value was reported.

The three-point bending tests of the specimens were performed at room temperature by using a Testometric Universal Tester M350-20kN at a crosshead speed of 5 mm/min. The span between loading points was 50 mm. At least five specimens were tested for each sample and mean value was reported.

## RESULTS AND DISCUSSION

### *Structural Characterization of OMMT*

FTIR was applied to confirm the successful modification of OMMT. The FTIR spectra of original Na-MMT and five OMMT are illustrated in Fig. 2 in which the bands appeared at 1,041 $cm^{-1}$, 520 $cm^{-1}$ and 470 $cm^{-1}$ are due to stretching frequency of Si—O, Al—O, and Mg—O, respectively, of Na-MMT. The broad band centered near 3,400 $cm^{-1}$ in Na-MMT (curve a) is due to —OH stretching vibration for interlayer water. And the overlaid absorption peak in the region of 1637 $cm^{-1}$ is assigned to the —OH bending mode of adsorbed water [43]. Compared with Na-MMT, the absorption bands at 1,723 $cm^{-1}$, 1,489 $cm^{-1}$, and 1,308 $cm^{-1}$ in M-MMT (curve b) are attributed to the C═O stretching vibration, N—H bending vibration and C—O stretching vibration, respectively, implying that MMT is successfully modified by MTC. In the same way, D-MMT (curve c) shows

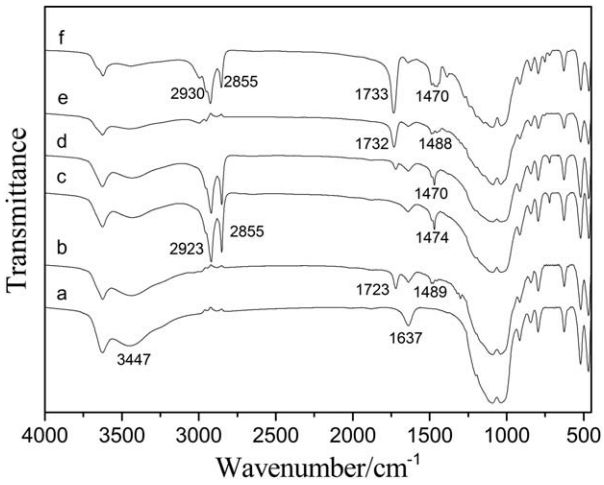


FIG. 2. FTIR spectra of original MMT and OMMTs (a) Na-MMT; (b) M-MMT; (c) D-MMT; (d) MD-MMT; (e) PgM-MMT; (f) PgMD-MMT.

peaks at 2,923 $cm^{-1}$, 2,855 $cm^{-1}$, and 1,474 $cm^{-1}$, which are due to stretching vibration and symmetric bending vibration of $-CH_2$ groups, thus indicating the effective organomodification of MMT by DODAC. Meanwhile, the spectrum of MD-MMT (curve d) is mainly a combination of M-MMT and D-MMT. These results indicate that the alkyl ammonium chains have been intercalated into the galleries of MMT by a cation-exchange reaction. In addition, the C=O stretching vibration absorption appeared near 1,730 $cm^{-1}$ becomes stronger in PgM-MMT and PgMD-MMT than in M-MMT and MD-MMT, which can be ascribed to the successful grafting of PMMA. Thus, the presence of organic groups in the organoclay indicated the successful modification of Na-MMT.

The WAXD patterns of original Na-MMT and five OMMT are displayed in Fig. 3. It is obvious that the diffraction peaks for all OMMT are shifted to smaller angles comparing with Na-MMT, indicating that all OMMT were successfully modified. Bragg's equation, $d = n\lambda/2\sin\theta$, was applied to calculate the interlayer spacing ($d_{001}$) of the samples by using θ-values from the WAXD patterns. The initial *d*-value of original MMT was determined to be 1.25 nm. After modification, the diffraction peaks of the OMMT shifted to a lower 2θ angle, representing an increase in interlayer spacing. The peak position and interlayer spacing results are summarized in Table 1. It is worth to note that there are some second peaks in the patterns of D-MMT, MD-MMT, and PgMD-MMT, which can be ascribed to the existence of OMMT with smaller interlayer spacing since not all the MMT could achieve the same fully-intercalated state even when the same organic modifier is applied. Nevertheless, the intensity of first peak in every diffractogram is far stronger than corresponding second peak, which manifest that most of the OMMT actually bared an average interlayer spacing corresponding to the first peak. Therefore, the existence of a second peak will not interfere with consequent discussions on the structure of OMMT and its effect on mechanical properties.

The differences of interlayer spacing can be attributed to the difference of organic modifier's chain length. Although MTC can provide functional groups (double bonds) that can react with monomers, the chain length of MTC is relatively short compared with DODAC. Therefore, MTC alone cannot expand the galleries effectively, only resulting in 0.2-nm interlayer expansion for M-MMT. And for PgM-MMT, the grafting reaction did not endow it with desired large interlayer *d*-spacing although, in theory, the growing of polymers in the galleries was expected to hugely increase the gallery height. This could be attributed to the fact that, in xylene solution where grafting reaction happened, the hydrophilic MMT layers tended to bundle with each other, thus making it difficult for chain propagation to take place in the limited interlayer spaces. Nonetheless, the *d*-spacing of PgM-MMT is still larger than M-MMT, implying that some PMMA chains did insert into the interlayer of MMTs after grafting reaction. In clear contrast to MTC, the long alkyl chains of DODAC make it possible to expand the gallery more sufficiently, thus achieving better intercalation effect. Consequently, D-MMT, MD-MMT and PgMD-MMT displayed higher interlayer spacing than M-MMT and PgM-MMT. Moreover, among D-MMT, MD-MMT and PgMD-MMT, PgMD-MMT possesses the largest interlayer spacing due to the combination of DODAC and MTC: DODAC was able to expand the interlayer effectively so that MMA could insert into the galleries to react with MTC, thus the chain length of modifiers could increase rapidly during the grafting reaction, giving rise to larger interlayer spacing. As shown in the table, the $d_{001}$ of PgMD-MMT is as much as 3.85 nm, which is 3-fold larger than that of original Na-MMT.

In conclusion, all five kinds of OMMT were successfully organomodified. The interlayer spacing of each OMMT was mainly determined by the modification agents utilized as well as the modification method

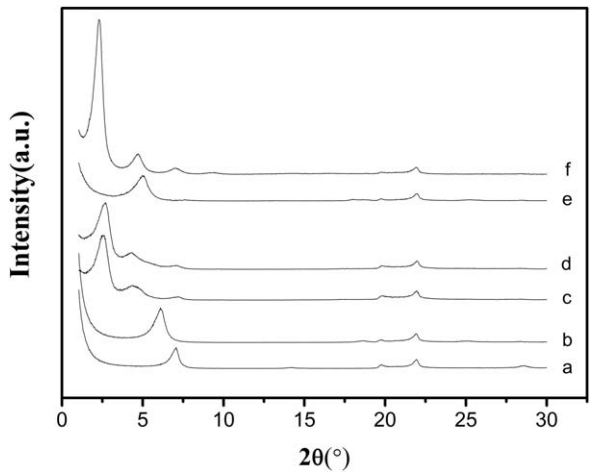


FIG. 3. WAXD patterns of original MMT and OMMTs (a) Na-MMT; (b) M-MMT; (c) D-MMT; (d) MD-MMT; (e) PgM-MMT; (f) PgMD-MMT.


DOI 10.1002/pc

TABLE 1. WAXD data for original MMT and five kinds of MMT.

| Sample | Peak position 2θ (°) | Interlayer spacing, $d_{001}$ (nm) | Interlayer expansion, $\Delta d_{001}$ (nm) |
|---|---|---|---|
| Na-MMT | 7.06 | 1.25 | – |
| M-MMT | 6.05 | 1.45 | 0.20 |
| D-MMT | 2.40 | 3.67 | 2.42 |
| MD-MMT | 2.66 | 3.35 | 2.10 |
| PgM-MMT | 4.98 | 1.77 | 0.52 |
| PgMD-MMT | 2.27 | 3.85 | 2.60 |

applied. The long alkyl chains of DODAC endow DODAC with the ability to expand the gallery more sufficiently. By comparison, although MTC alone cannot expand the galleries effectively due to their short chain length, the double bond groups on MTC make it possible to conduct subsequent grafting reaction, which can lead to larger interlayer spacing. As a result, it turned out that the PgMD-MMT possessed the maximum interlayer spacing among all five kinds of OMMT.

### *Structural Characterization of PMMA/OMMT Nanocomposites Microspheres*

Polymer–clay nanocomposites could be characterized as immiscible (tactoids), intercalated, partially exfoliated, or exfoliated. The particular form depends on the clay content, the chemical nature of the organic modifier, and the synthetic method. In general, an exfoliated system is more feasible with lower clay content (about 1 wt%), while an intercalated structure is frequently observed for nanocomposites with higher clay content [23]. Therefore, the PMMA/OMMT nanocomposites with different OMMT were all studied at an OMMT loading of 1 wt%. In addition, after excluding the influence of clay content and synthetic method, the modification of MMT becomes the decisive factor determining the structure of PMMA/OMMT nanocomposites studied in this article.

WAXD results for all PMMA/OMMT nanocomposites microspheres are shown in Fig. 4. In particular, no significant peak corresponding to $d_{001}$ was found for PMMA/PgM-MMT (curve d) and PMMA/PgMD-MMT (curve e). As a result, it is suggested that these products are mainly exfoliated. However, weak peaks around $2\theta = 1.9°$, 2.0°, and 1.8°, corresponding to $d_{001} = 4.64$, 4.41, and 4.90 nm, were detected for PMMA/M-MMT (curve a), PMMA/D-MMT (curve b) and PMMA/MD-MMT (curve c), respectively. Comparing the above $d_{001}$ spacing value of the nanocomposites to the respective values of M-MMT (1.45 nm), D-MMT (3.67 nm) and MD-MMT (3.35 nm), it is obvious that the diffraction peaks of OMMT are shifted to lower angles, resulting from the partially exfoliated and partially intercalated structure of obtained nanocomposites.

As is well known, the mostly used modifiers for MMT are cationic surfactants with long organic chains, which can be tethered to the surface of MMT layers, resulting in an increase of the gallery height. Sometimes, the modifiers may even provide functional groups that can react with the polymer or initiate polymerizaion of monomers [44]. The surface modification of MMT both increases the basal spacing of clays and serves as a compatibilizer between the hydrophilic clay and the hydrophobic polymer [45]. That is to say, the interlayer spacing and the compatibility between two phases are two important factors affecting the intercalation of polymer molecules, which in turn determines the final structure of polymer/MMT nanocomposites.

In our work, D-MMT, MD-MMT and PgMD-MMT all possessed relatively large interlayer spacing due to the existence of DODAC, but only PMMA/PgMD-MMT obtained an exfoliated structure after in situ suspension polymerization. It is because, in the case of PgMD-MMT, PMMA chains were adsorbed onto the surface of MMT after the grafting reaction, thus increasing the compatibility between PgMD-MMT and PMMA matrix. Consequently, it is very easy for MMA monomers to diffuse into the galleries to initiate chain propagation or for PMMA molecules to insert into interlayer spacing. Either way, the exfoliation of MMT layers is more likely to take place. However, for D-MMT and MD-MMT, the nonpolar long alkyl chains of DODAC are not very compatible with polar MMA monomers or PMMA chains. Accordingly, the intercalation of D-MMT and MD-MMT is not as easy as in the case of PgMD-MMT, merely resulting in partially exfoliated and partially intercalated structures.

On the other hand, for PMMA/M-MMT nanocomposites, a partially exfoliated and partially intercalated structure was achieved in despite of a short 1.45 nm *d*-spacing for M-MMT. This result could be attributed to the existence of double bonds. What seems particularly surprising is that PgM-MMT overcame its short interlayer spacing and attained an exfoliated dispersion in PMMA/PgM-MMT nanocomposites. Again, this phenomenon could be

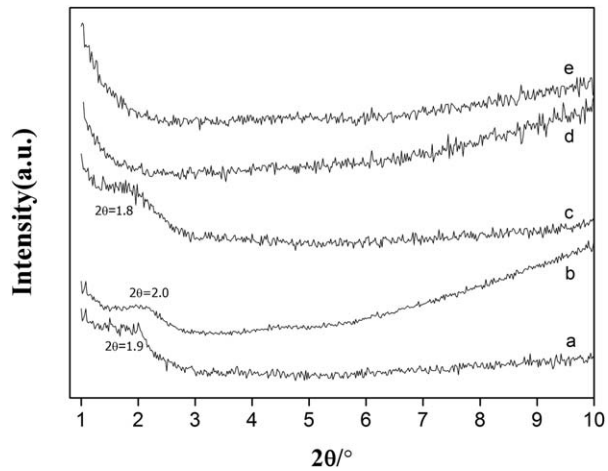


FIG. 4. WAXD patterns of all PMMA/OMMT nanocomposites (a) PMMA/M-MMT; (b) PMMA/D-MMT; (c) PMMA/MD-MMT; (d) PMMA/PgM-MMT; (e) PMMA/PgMD-MMT.

ascribed to the incredible compatibility induced by grafted PMMA polymers. What's more, as discussed above, the growing of PMMA within the PgM-MMT galleries was restrained during the grafting reaction due to a limited space. Therefore, it is reasonable to speculate that there still were some unreacted double bond groups after the grafting process. In other words, the coexistence of unreacted MTC, which could provide reactive groups to participate in chain propagation, and grafted PMMA polymers, which could improve the compatibility between two phases to make it easier for monomers to diffuse into galleries, may be responsible for the exfoliated dispersion of PgM-MMT in PMMA matrix.

In conclusion, the WAXD results could reliably indicate the compatibility of each kind of OMMT to PMMA matrix. On the other hand, large interlayer spacing of OMMT could not entirely ensure an exfoliated structure in PMMA/MMT microspheres, while OMMT with relative small $d_{001}$ could still yield exfoliated structure as long as the compatibility between OMMT and polymer matrix was favorable.

### *Molecular Weight Determination*

The weight and number average molecular weight ($\overline{Mw}$ and $\overline{Mn}$) as well as the polydispersity index (PDI) of pure PMMA and all PMMA nanocomposites are represented in Table 2. In this article, the molecular weight of PMMA/OMMT nanocomposites refers to the molecular weight of extracted PMMA from corresponding nanocomposites. As shown in the table, all the PMMA/OMMT nanocomposites exhibit lower molecular weight values than neat PMMA, while the PDI of all nanocomposites are larger than that of neat PMMA. Generally, when the MMA monomers are attracted into the intragallery of clay layer, the polymerization process was interrupted by the clay structure. Therefore, the molecular weight tends to decrease [30] and PDI becomes larger. According to Table 2, it is worthwhile to point out that the grafting process of OMMT can remarkably raise the molecular weight of PMMA polymers in corresponding nanocomposites, although the $\overline{Mw}$ and $\overline{Mn}$ of PMMA/PgM-MMT and PMMA/PgMD-MMT are still slightly lower than those of neat PMMA. Indeed, the modification method of MMT would have an impact on the in situ suspension polymerization of PMMA/OMMT nanocomposites. However, since such small molecular weight change itself will not affect the mechanical properties of the composites significantly, we did not study how the OMMT affects the polymerization in detail.

TABLE 2. Molecular weight measurements (weight average molecular weight $\overline{Mw}$, number average molecular weight $\overline{Mn}$, and polydispersity index PDI) for pure PMMA and PMMA/OMMT nanocomposites.

| Sample | $\overline{Mw}$ ($\times 10^4$) | $\overline{Mn}$ ($\times 10^4$) | PDI |
|---|---|---|---|
| pure PMMA | 91.6 | 37.6 | 2.44 |
| PMMA/M-MMT | 74.7 | 25.9 | 2.88 |
| PMMA/D-MMT | 64.9 | 20.1 | 3.23 |
| PMMA/MD-MMT | 70.9 | 20.9 | 3.39 |
| PMMA/PgM-MMT | 90.3 | 33.0 | 2.74 |
| PMMA/PgMD-MMT | 84.2 | 31.3 | 2.69 |

### *Mechanical Properties*

**Tensile Properties.** The effect of the different OMMT type on the tensile properties such as Young's modulus, tensile strength and strain at break was investigated, and the results are depicted in Fig. 5. It can be seen clearly from Fig. 5 that all nanocomposites exhibited higher Young's modulus than neat PMMA. The enhancement of modulus is reasonably attributed to the reinforcement effect of the rigid inorganic clay and the constraining effect of silicate layers on molecular motion of polymer molecular chains [4, 46, 47]. Particularly, an augmentation of 24.4% and 15.5% in Young's modulus for PMMA/PgM-MMT and PMMA/PgMD-MMT was observed, respectively, much larger than PMMA/M-MMT, PMMA/D-MMT, and PMMA/MD-MMT. The higher values of Young's modulus of the nanocomposites with PgM-MMT and PgMD-MMT could be attributed to the better compatibility of OMMT with the organic phase due to the existence of grafted PMMA polymer chains, resulting in exfoliated structure and a more homogeneous OMMT dispersion into the PMMA matrix. On the other hand, according to previous report that exfoliation degree of layered silicate in polymer matrix is responsible for improving properties of polymer/layered silicate nanocomposites 23, 29, 48, it can be speculated that the extent of improvement of Young's modulus for M-MMT, D-MMT, and MD-MMT was also related to their exfoliation degree in the polymer matrix.

Here, it is worth to note that the Young's modulus of PMMA/PgM-MMT was higher than that of PMMA/PgMD-MMT, although PgMD-MMT possessed the maximum interlayer spacing among all OMMT before being incorporated into PMMA matrices. This interesting phenomenon could be ascribed to the discrepancy in compatibility between organic modifiers and PMMA matrices. For PMMA/PgM-MMT and PMMA/PgMD-MMT, which both attained an exfoliated structure, the interfacial adhesion between OMMT and PMMA matrices plays a decisive role on the mechanical properties of nanocomposites. And in our work, the interfacial adhesion between OMMT and PMMA matrices was mainly determined by the compatibility between organic modifiers and PMMA matrices. In PMMA/PgM-MMT, the MTC modifiers tethered on the surface of MMT all reacted with MMA monomers either in the grafting reaction or during the in situ polymerization. In both cases, strong interaction between PgM-MMT and PMMA matrix came about and, therefore, better dispersion of PgM-MMT was more likely to occur. On the contrary, DODAC, with its nonpolar long alkyl chains,

 DOI 10.1002/pc

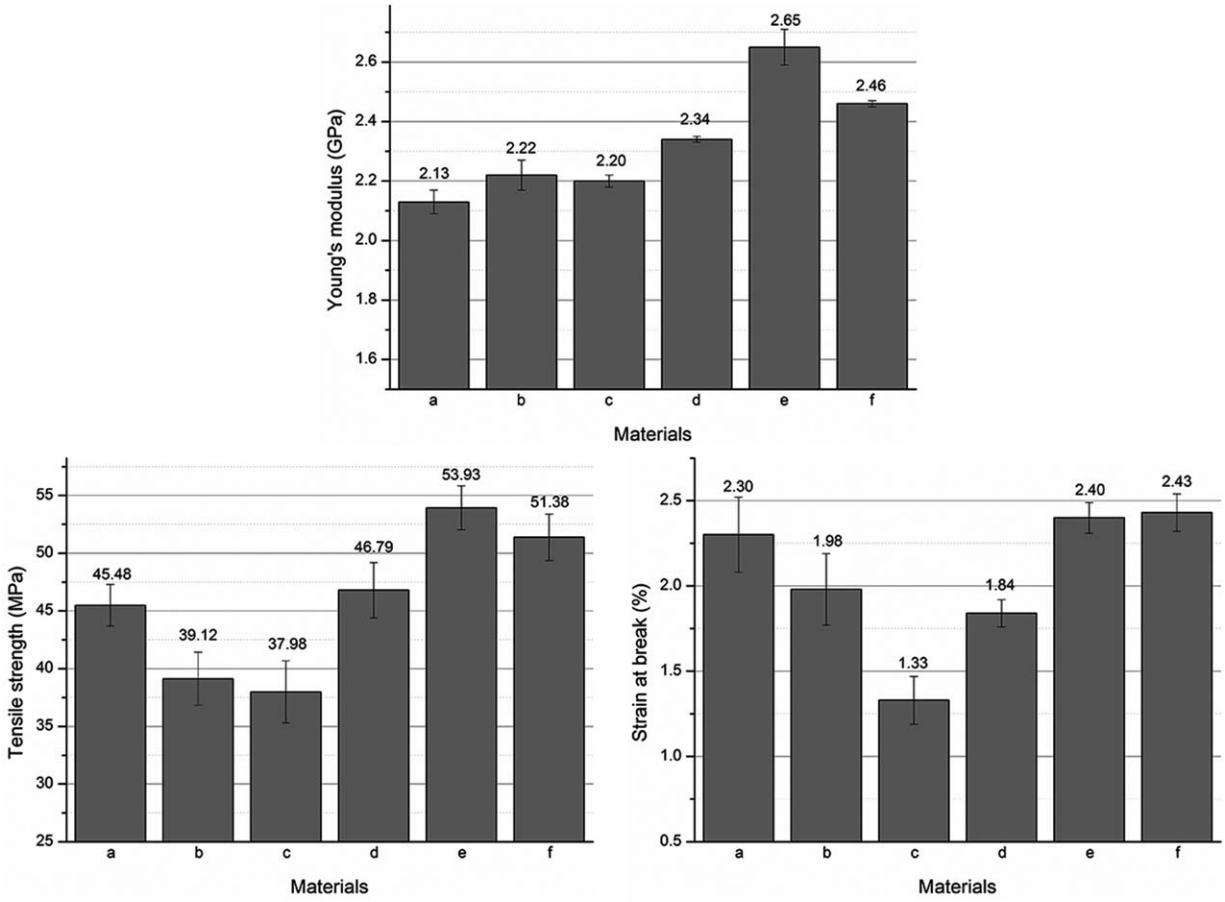


FIG. 5. Tensile properties of pure PMMA and PMMA/OMMT nanocomposites. (a) pure PMMA; (b) PMMA/M-MMT; (c) PMMA/D-MMT; (d) PMMA/MD-MMT; (e) PMMA/PgM-MMT; (f) PMMA/PgMD-MMT.

possessed relatively inferior compatibility with polar PMMA matrices. Therefore, the interfacial adhesion between PgMD-MMT and PMMA matrix was not as strong as in the case of PgM-MMT and the Young's modulus of PMMA/PgMD-MMT was lower than that of PMMA/PgM-MMT. In conclusion, the fact that PMMA/PgM-MMT nanocomposite turned out to have the highest Young's modulus despite PgM-MMT only possessed a short interlayer spacing indicates that the compatibility between OMMT and PMMA matrix, other than *d*-spacing of OMMT, is the dominant factor deciding the final mechanical properties of PMMA/MMT nanocomposites.

In Fig. 5, it can also be observed that the tensile strength increased only for PMMA/MD-MMT, PMMA/PgM-MMT, and PMMA/PgMD-MMT. The incorporation of M-MMT and D-MMT did not improve the tensile strength of PMMA matrix, which could be attributed to the poor dispersion of M-MMT and D-MMT. Unlike in the case of Young's modulus, the addition of organic nanofillers cannot ensure an improvement on tensile strength because either bad dispersion or poor interfacial adhesion will lead to a deterioration of strengths. Nikolaidis et al. reported the synthesis of PMMA/OMMT nanocomposites by in situ bulk polymerization with seven kinds of OMMT. It turned out that more than half of the OMMT failed to enhance the tensile strength of PMMA matrices [23]. And for MD-MMT, although it had higher exfoliation degree than M-MMT and D-MMT, it was still partilly exfoliated and partially intercalated in the PMMA/MD-MMT nanocomposite. Therefore, the improvement of tensile strength was limited for PMMA/MD-MMT. In contrast, the PMMA/PgM-MMT nanocomposite showed the highest tensile strength followed by PMMA/PgMD-MMT nanocomposite. This could be ascribed to the higher degree of exfoliation in these nanocomposites. When the clay particles are dispersed more finely (exfoliated), we can get a higher aspect ratio of the dispersed particles and a larger interfacial area, both of which make stress transfer to the silicate layers much more effective; this will lead to improvements of the tensile strength [49].

On the other hand, the strain at break increased a little for PMMA/PgM-MMT and PMMA/PgMD-MMT nanocomposites, while M-MMT, D-MMT, and MD-MMT imparted inferior values to PMMA. One of the factors which contribute to losses in strain at break is the

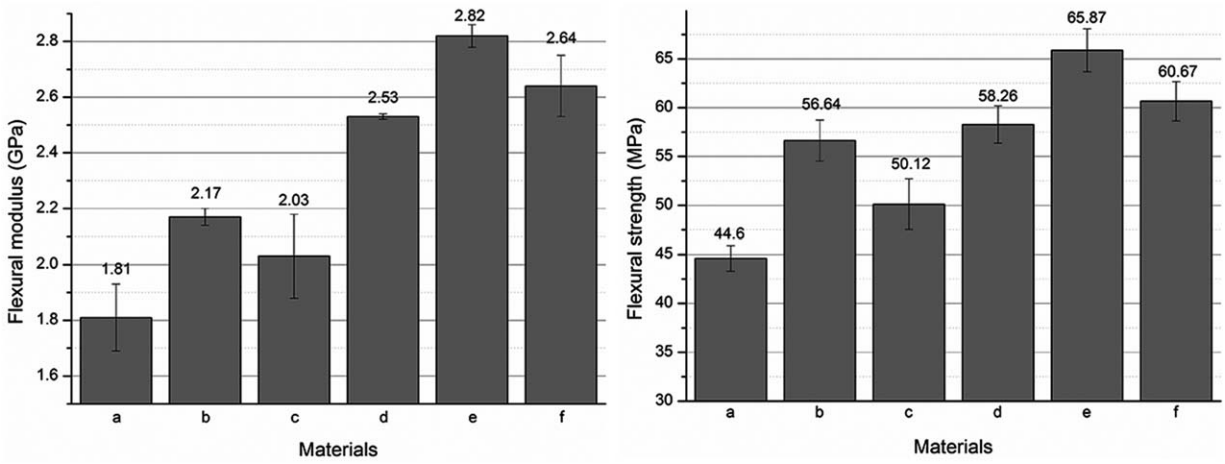


FIG. 6. Flexural properties of pure PMMA and PMMA/OMMT nanocomposites (a) pure PMMA; (b) PMMA/M-MMT; (c) PMMA/D-MMT; (d) PMMA/MD-MMT; (e) PMMA/PgM-MMT; (f) PMMA/PgMD-MMT.

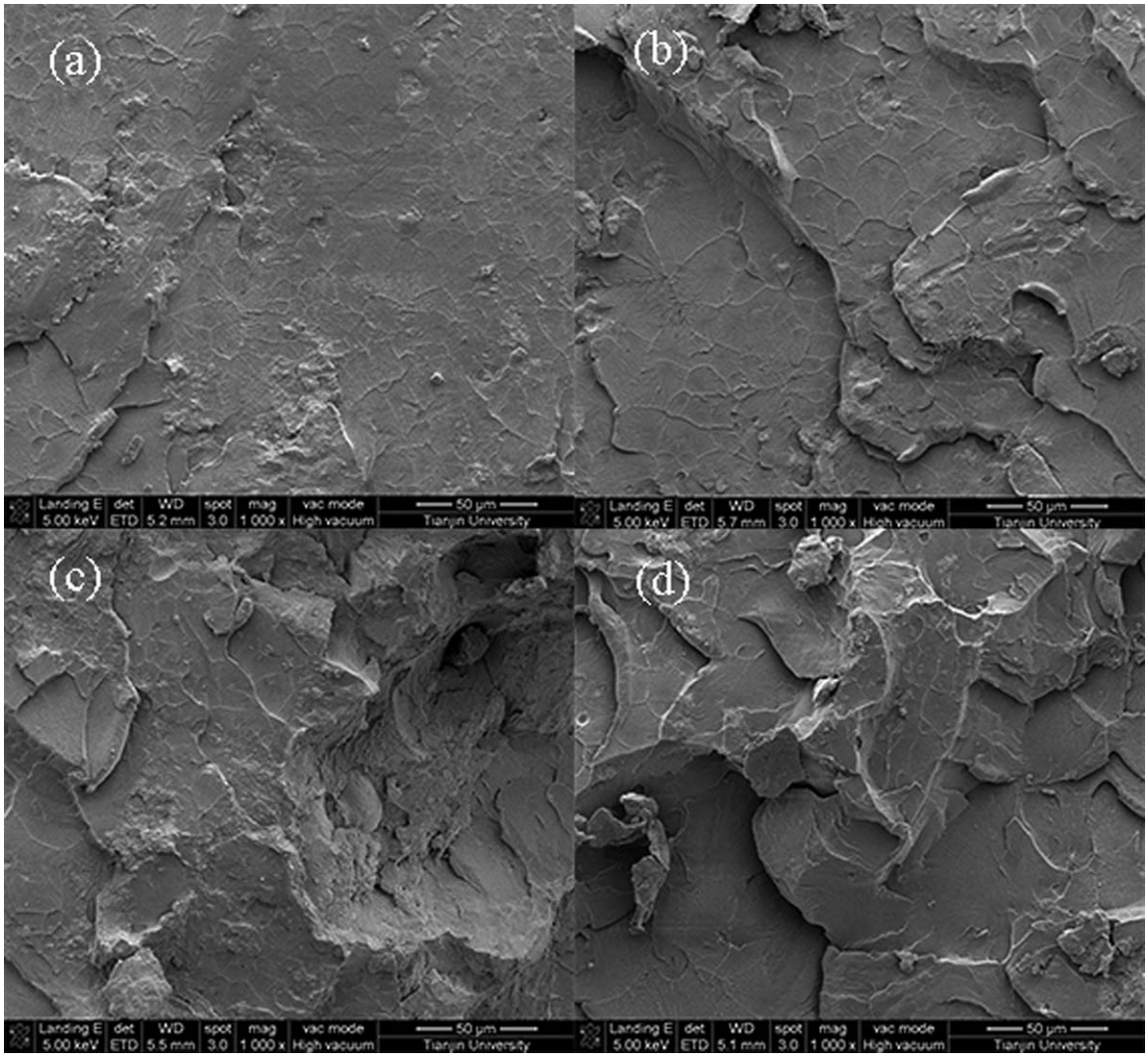


FIG. 7. SEM images of tensile fractured surface of (a) pure PMMA, (b) PMMA/M-MMT, (c) PMMA/D-MMT and (d) PMMA/PgM-MMT.

 DOI 10.1002/pc

exfoliation degree of the MMT in nanocomposites. The tactoids from some possible unexfoliated platelets of M-MMT, D-MMT and MD-MMT can act as stress concentrators thus contributing to loss in strain at break [49]. In comparison, the increase of strain at break for PMMA/PgM-MMT and PMMA/PgMD-MMT nanocomposites could be explained on the basis of higher extents of exfoliation as well as the stronger interactions between the polar PMMA chains and the polar silicate surface [50].

**Flexural Properties.** Besides tensile performance, the flexural properties of virgin PMMA and PMMA/OMMT nanocomposites were also investigated. Figure 6 demonstrates the flexural properties such as flexural modulus and flexural strength of neat PMMA and PMMA/OMMT nanocomposites. A similar trend to that of the Young's modulus can be observed for flexural modulus. The incorporation of all kinds of OMMT increased the flexural modulus and flexural strength remarkably, which could be attributed to high stiffness and aspect ratio of silicate [51]. Among all samples, the PMMA/PgM-MMT exhibited the highest flexural modulus and strength as shown on tensile properties. Compared with neat PMMA, the flexural modulus and flexural strength of PMMA/PgM-MMT were increased by 55.8% and 47.69%, respectively. This could again be associated with the better dispersion and exfoliation of PgM-MMT in PMMA matrix as well as the superior compatibility between PgM-MMT and PMMA matrix.

*Tensile Fracture Surfaces*

Figure 7 depicts the SEM images of tensile fractured surface of pure PMMA and some PMMA/OMMT nanocomposites specimens (PMMA/M-MMT, PMMA/D-MMT, and PMMA/PgM-MMT). It is evident from Fig. 7 that pure PMMA possesses a typical smooth fracture surface morphology with very few defects or voids. In contrast, all the fracture surfaces of PMMA/OMMT were rough, revealing that OMMT could produce effective physical interaction and reduce the slippage of OMMT nanoparticles. These phenomena could well explain the enhancement of mechanical properties upon the incorporation of OMMT.

## CONCLUSIONS

In this investigation, five kinds of OMMT were successfully prepared and then PMMA/OMMT nanocomposites were prepared by in situ suspension polymerization. WAXD results indicated the formation of exfoliated structure for the nanocomposites microspheres containing PgM-MMT and PgMD-MMT, whereas a mixture of intercalated and exfoliated structures for the nanocomposites microspheres containing M-MMT, D-MMT, and MD-MMT. The incorporation of all five kinds of OMMT increased the Young's modulus, while only the tensile strength of nanocomposites with PgM-MMT and PgMD-MMT was enhanced obviously due to their high compatibility between matrix and OMMT clays. On the other hand, the flexural property, including flexural modulus and flexural strength, for all PMMA/OMMT nanocomposites increased remarkbly. Among all samples, the PMMA/PgM-MMT nanocomposite exhibited the best mechanical properties. This could be associated with the better dispersion and exfoliation of PgM-MMT in PMMA matrix as well as the superior compatibility between PgM-MMT and PMMA matrix.

## NOMENCLATURE

| | |
|---|---|
| BPO | Benzoyl peroxide |
| DODAC | Dioctadecyl dimethyl ammonium chloride |
| FTIR | Fourier transform infrared spectroscopy |
| GPC | Gel permeation chromatograph |
| HEC | Hydroxylethyl cellulose |
| MMT | Montmorillonite |
| MTC | Methacrylatoethyltrimethyl ammonium chloride |
| OMMT | Organomodified MMT |
| PMMA | Poly(methyl methacrylate) |
| SDBS | Sodium dodecyl benzene sulfonate |
| WAXD | Wide angle X-ray diffraction |

## REFERENCES


1. B. Chen, J.R.G. Evans, H.C. Greenwell, P. Boulet, P.V. Coveney, A.A. Bowden, and A. Whiting, *Chem. Soc. Rev.*, **37**, 568 (2008).
2. A. Okada and A. Usuki, *Macromol. Mater. Eng.*, **291**, 1449 (2006).
3. V. Mittal, *Materials*, **2**, 992 (2009).
4. S. Pavlidou and C.D. Papaspyrides, *Prog. Polym. Sci.*, **33**, 1119 (2008).
5. G. Choudalakis and A.D. Gotsis, *Eur. Polym. J.*, **45**, 967 (2009).
6. P. Kiliaris and C.D. Papaspyrides, *Prog. Polym. Sci.*, **35**, 902 (2010).
7. A.A. Azeez, K.Y. Rhee, S.J. Park, and D. Hui, *Compos. Part B-Eng.*, **45**, 308 (2013).
8. J. Soulestin, B.J. Rashmi, S. Bourbigot, M.-F. Lacrampe, and P. Krawczak, *Macromol. Mater. Eng.*, **297**, 444 (2012).
9. Q. Tai, X. Shan, L. Song, S. Lo, R.K.K. Yuen, and Y. Hu, *Polym. Compos.*, **35**, 167 (2014).
10. B. Tang, D. Cai, J. Sun, J. Wang, and L. Dai, *Polym. Compos.*, **34**, 2076 (2013).
11. K. Alena, M. Dagmar, G.J. Francois, and S. Miroslav, *Polym. Compos.*, **34**, 1418 (2013).
12. K. Prakalathan, S. Mohanty, and S.K. Nayak, *Polym. Compos.*, **35**, 999 (2014).
13. J. Ma, M. Lu, C. Cao, and H. Zhang, *Polym. Compos.*, **34**, 626 (2013).
14. E.A. Stefanescu, X. Tan, Z. Lin, N. Bowler, and M.R. Kessler, *Polymer*, **51**, 5823 (2010).
15. M.L. Hernandez, L.M. Alonso, M.M. Pradas, O.E.L. Lozano, and D.G. Bello, *Polym. Compos.*, **34**, 1927 (2013).

16. J.-M. Yeh, S.-J. Liou, C.-Y. Lin, C.-Y. Cheng, and Y.-W. Chang, *Chem. Mater.*, **14**, 154 (2002).
17. M. Huskić and M. Žigon, *Eur. Polym. J.*, **43**, 4891 (2007).
18. L. Martin, G. Kortaberria, A. Vazquez, M. Fermeglia, L. Martinelli, S. Sinesi, A. Jimeno, K. de la Caba, and I. Mondragon, *Polym. Compos.*, **29**, 782 (2008).
19. P.K. Sahoo and R. Samal, *Polym. Degrad. Stab.*, **92**, 1700 (2007).
20. P. Pandey, S. Anbudayanidhi, S. Mohanty, and S.K. Nayak, *Polym. Compos.*, **33**, 2058 (2012).
21. Y. Xu, W.J. Brittain, C. Xue and R.K. Eby, *Polymer*, **45**, 3735 (2004).
22. K.-C. Chang, S.-T. Chen, H.-F. Lin, C.-Y. Lin, H.-H. Huang, J.-M. Yeh, and Y.-H. Yu, *Eur. Polym. J.*, **44**, 13 (2008).
23. A.K. Nikolaidis, D.S. Achilias, and G.P. Karayannidis, *Eur. Polym. J.*, **48**, 240 (2012).
24. M. Huskić, E. Žagar, and M. Žigon, *Eur. Polym. J.*, **48**, 1555 (2012).
25. H. Essawy, A. Badran, A. Youssef, and A.E. Abd El-Hakim, *Polym. Bull.*, **53**, 9 (2004).
26. X. Zheng, D.D. Jiang, and C.A. Wilkie, *Thermochim. Acta*, **435**, 202 (2005).
27. M. Si, M. Goldman, G. Rudomen, M.Y. Gelfer, J.C. Sokolov, and M.H. Rafaiiovich, *Macromol. Mater. Eng.*, **291**, 602 (2006).
28. M.U. Khan, V.G. Gomes, and I.S. Altarawneh, *Carbon*, **48**, 2925 (2010).
29. A.K. Nikolaidis, D.S. Achilias, and G.P. Karayannidis, *Ind. Eng. Chem. Res.*, **50**, 571 (2011).
30. T.-Y. Tsai, C.-K. Wen, H.-J. Chuang, M.-J. Lin, and U. Ray, *Polym. Compos.*, **30**, 1552 (2009).
31. Q. Kong, Y. Hu, L. Yang, and W. Fan, *Polym. Compos.*, **27**, 49 (2006).
32. W.S. Wang, C.K. Liang, Y.C. Chen, Y.L. Su, T.Y. Tsai, and Y.W. Chen-Yang, *Polym. Adv. Technol.*, **23**, 625 (2012).
33. W. Wei, E. Abdullayev, A. Hollister, D. Mills, and Y.M. Lvov, *Macromol. Mater. Eng.*, **297**, 645 (2012).
34. A. Bettencourt and A.J. Almeida, *J. Microencapsul.*, **29**, 353 (2012).
35. N. Misra, G. Kapusetti, S. Jaiswal, and P. Maiti, *J. Appl. Polym. Sci.*, **121**, 1203 (2011).
36. J.-H. Wang, T.-H. Young, D.-J. Lin, M.-K. Sun, H.-S. Huag, and L.-P. Cheng, *Macromol. Mater. Eng.*, **291**, 661 (2006).
37. N. Salahuddin, *Polym. Compos.*, **30**, 13 (2009).
38. N. Salahuddin and M.M. Shehata, *Mater. Lett.*, **52**, 289 (2002).
39. X. Huang and W.J. Brittain, *Macromolecules*, **34**, 3255 (2001).
40. N. Clarke, L.R. Hutchings, I. Robinson, J.A. Elder, and S.A. Collins, *J. Appl. Polym. Sci.*, **113**, 1307 (2009).
41. J. Zheng, Q. Su, C. Wang, G. Cheng, R. Zhu, J. Shi, and K. Yao, *J. Mater. Sci.: Mater. Med.*, **22**, 1063 (2011).
42. X. Wang, Q. Su, Y. Hu, C. Wang, and J. Zheng, *J. Therm. Anal. Calorim.*, **115**, 1143 (2014).
43. Y. Bao, J. Ma, and N. Li, *Carbohydr. Polym.*, **84**, 76 (2011).
44. I.-J. Chin, T. Thurn-Albrecht, H.-C. Kim, T.P. Russell, and J. Wang, *Polymer*, **42**, 5947 (2001).
45. A.S. Zerda and A.J. Lesser, *J. Polym. Sci. Polym. Phys.*, **39**, 1137 (2001).
46. Z.Z. Yu, C. Yan, M. Yang, and Y.W. Mai, *Polym. Int.*, **53**, 1093 (2004).
47. T. Liu, W.C. Tjiu, C. He, S.S. Na, and T.S. Chung, *Polym. Int.*, **53**, 392 (2004).
48. Z.A. Kusmono, W.S. Mohd Ishak, T. Chow, Takeichi, and Rochmadi, *Polym. Compos.*, **31**, 1156 (2004).
49. J.W. Lee, M.H. Kim, W.M. Choi, and O.O. Park, *J. Appl. Polym. Sci.*, **99**, 1752 (2006).
50. M. Alexandre and P. Dubois, *Mater. Sci. Eng. R Rep.*, **28**, 1 (2000).
51. S. Parija, S.K. Nayak, S.K. Verma, and S.S. Tripathy, *Polym. Compos.*, **25**, 646 (2004).

 DOI 10.1002/pc